Effect of Low-Temperature Plasma Activated Water with Different Treatment Times on Myofibrillar Proteins of Thawed Pork

Manting Du , Fangge Hao , Shunyang Sun , Ke Li , Qisen Xiang , Junguang Li , Lichuang Cao , Yanhong Bai *

Posted Date: 18 February 2025

doi: 10.20944/preprints202502.1353.v1

Keywords: plasma-activated water; thawed pork; myofibrillar proteins; gelation properties

Article

Effect of Low-Temperature Plasma Activated Water with Different Treatment Times on Myofibrillar Proteins of Thawed Pork

Manting Du [1,2], Fangge Hao [1], Shunyang Sun [1], Ke Li [1,2], Qisen Xiang [1,2], Junguang Li [1,2], Lichuang Cao [1,2] and Yanhong Bai [1,2,*]

[1] College of Food and Bioengineering, Zhengzhou University of Light Industry, Zhengzhou, 450001, China

[2] Key Laboratory of Cold Chain Food Processing and Safety Control, Ministry of Education, Zhengzhou University of Light Industry, Zhengzhou, 450001, China

* Correspondence: baiyanhong212@163.com (Y.B.).

Abstract: In this study, myofibrillar proteins (MPs) of thawed pork were treated with plasma-activated water (PAW) for diverse durations (0, 5, 10, 15, 20, and 25 s) to investigate whether the function of MPs improved by PAW and the corresponding regulatory mechanism. The results found that PAW treatments increased the surface hydrophobicity, altered secondary and tertiary structure of MPs. The α-helix content of MPs treated by PAW reduced from 37.3% to 31.25%. In PAW25s group, the oxidation of MPs significantly raised reflected by the higher carbonyl content and lower total sulfhydryl content compared to other groups (P<0.05). Furthermore, PAW treatments increased the whiteness, improved the strength, immobilized water contents, resilience, chewiness, and adhesiveness of MP gels. The observation of intermolecular forces and microstructure of MP gels presented the increase in ionic bonding, disulfide bonding, and hydrophobic interactions, but decrease in hydrogen bonding in MP gels with PAW treatments, leading to more homogeneous and denser gel structures compared to control group. In conclusion, PAW treatment for a short duration significantly fixed and enhanced the function of MPs extracted from thawed pork, and to some extent, improved the processing quality of MPs of thawed pork.

Keywords: plasma-activated water; thawed pork; myofibrillar proteins; gelation properties

1. Introduction

Freezing serves as an essential way to extend the shelf life of meat products. It delays the deterioration of meat quality, reduces biochemical reactions, and inhibits microbial growth in meat [1]. However, during the freezing process, majority of water in pork turned to ice crystals, which severely damage the tissue structure of pork, leading to the losses of thawing juices and the further deterioration of qualities of pork [2]. As the main content of muscle, myofibrillar proteins (MPs) easily damaged by the generation of ice crystals during freezing, causing the deterioration of MP properties after thawing. Consequently, the development of new technologies to fix and improve the structure and functions of MPs of thawed meat will have a profound impact on the better utilization of thawed meat.

Low-temperature plasma-activated water (LT-PAW) usually generated by plasma jet gun charging directly under ionizing distilled water with high pressure or treating distilled water indirectly using dielectric blocking discharge (DBD), sliding arc, and other media [3]. LT-PAW contains a lot of active substances, including NO^{2-}, NO^{3-}, H_2O_2, reactive oxygen and nitrogen species (RONS) [4,5]. In recent years, LT-PAW has been gradually applied to food industry, particularly to food preservation and sterilization. Li et al. [6] investigated the effect of PAW on the aggregation degree and gelation properties of myofibrillar proteins of Aristichthys nobilis and found that, as the PAW treatment time increased from 0 s to 240 s, the pH value of MPs decreased from 5.91 to 2.61.

 doi:10.20944/preprints202502.1353.v1

Simultaneously, PAW significantly enhanced the hydrophobic interactions of MPs, but weakened ionic bonding, aggregation and gelation of MPs, the structure of MPs changed by PAW treatment and finally improved the three-dimensional network structure and the gelation density of MPs gels. Qian et al. [7] prepared MPs gels with PAW and discovered that the gels treated by PAW had intrinsic antimicrobial activity.

Currently, research on LT-PAW mainly concentrates on the sterilization and preservation of noodles, vegetables, and meat products [8]. The potential ability of LT-PAW on changing the functions of MPs remains development. Besides, the problem of the decreases of MPs properties of thawed meat still needs more solutions. Thus, this study aims to verify the effect of LT-PAW on MPs of thawed pork and illustrate the relative mechanism by evaluating the changes of structure and gelation properties of MPs after PAW treatments, expecting to provide theoretical guidance for the application of LT-PAW in improving the processing quality of thawed pork.

2. Materials and Methods

2.1. Materials

The *longissimus lumborum* muscles of pork were procured from a local farmer's market in Zhengzhou City and transported to laboratory in a temperature range of 0 to 4°C. After transportation, the surface connective tissue and fat of pork were removed and then stored at -20°C for 72 h.

2.2. Preparation of PAW

Plasma generator was used to prepare PAW as described by Qian et al. [7]. PBS (0.6 mol/L NaCl, pH 7.0) buffer was pre-cooled to 4°C in advance and divided into six portions of 300 mL each. Then the plasma jet guns were placed approximately 5 cm below the pre-cooled PBS buffer and treated PBS buffer for durations of 0 s, 5 s, 10 s, 15 s, 20 s, and 25 s, respectively.

2.3. Extraction of MPs and PAW Treatment

MPs were extracted as described of Zhu et al. [9] with slight modifications. Firstly, the thawed pork were minced by a meat grinder and added with 4 times volume (m:v) of extraction solution 1 (10 mmol/L Na_2HPO_4/NaH_2PO_4, 0.1 mol/L NaCl, 2 mmol/L $MgCl_2$, 0.1 mol/L EGTA, pH 7.0, 4 °C). Then the mixture was homogenized under the condition of 10,000 r/min for 2 min. Homogenate centrifuged at 4 °C, 3000 g for 15 min, discarded supernatant and repeated three times. After that, the obtained sediment was mixed with 4 times the volume (m:v) of 0.1 mol/L NaCl wash solution, homogenized and centrifuged three times using previous conditions to obtain purified MPs.

MPs concentration was measured by Biuret method and adjusted with PBS buffer (50 mmol/L Na_2HPO_4/NaH_2PO_4, 0.6 mol/L NaCl, pH 7.0, 4 °C). Subsequently, the prepared 0 s, 5 s, 10 s, 15 s, 20 s, and 25 s PAW was mixed with MPs and named CK (0s), PAW5s (5s), PAW10s (10s), PAW15s (15s), PAW20s (20s), and PAW25s (25s), respectively.

2.4. Surface Hydrophobicity Measurement of Carbonyl Value

The surface hydrophobicity of MPs was determined by the bromophenol blue binding method (BPB) as described by Li et al. [10]. The concentration of MPs was diluted to 2 mg/mL. And 1 mL of the MPs was mixed with 40 μL of 1 mg/mL BPB solution and fully reacted at room temperature. After the reaction, the mixture was centrifuged at 6000 r/min, 4°C for 15 min and the supernatant was collected. The absorbance was tested at 595 nm using UV spectrophotometer (TU1810, Beijing General Instrument Co., Ltd., China).

$$\text{BPB bound } (\mu g) = \frac{(40\ \mu L \times A\_control - A\_sample)}{A\_control} \quad (1)$$

2.5. Ultraviolet Spectroscopy

 doi:10.20944/preprints202502.1353.v1

Deionized water was used as a blank, the concentration of MPs was diluted to 1 mg/mL. and the absorbance of sample was detected by UV spectrophotometer. The measurement range was from 200 to 360 nm.

2.6. Fluorescence Spectroscopy

The tertiary structure of MP was determined by fluorescence chromatography (F-7000, HITACHI, Japan). The concentration of MPs was diluted to 0.1 mg/mL. The settings of fluorescence spectroscopy parameters were as follows: excitation wavelength of 280 nm, emission wavelength range of 300 - 460 nm, slit width of 2.5 nm for all, and scanning rate of 12000 nm/min.

2.7. Sodium Dodecyl Sulfate-Polyacrylamide gel Electrophoresis (SDS-PAGE)

MPs compositional changes were measured using SDS-PAGE under non-reducing and reducing conditions, respectively, as described by Liu et al. [11]. Under reducing conditions, protein samples were mixed in equal volumes with loading buffer (0.5 mol/L Tris-HCl, 10% (w/v) SDS, 20% (v/v) glycine, 3.33% (w/v) dithiothreitol (DTT), 2% (w/v) bromophenol blue), boiled in water bath at 100°C for 5 min, and centrifuged at 13,000 r/min for 1 min. After that, 5 μL of supernatant was loaded into well. The concentrations of separating and concentrating gels were 10% and 5%. Under non-reducing conditions, there was no DTT in the loading buffer. Electrophoresis was performed at 70 V for separating gels and 110 V for concentrating gels. Gels were stained with Thomas Brilliant Blue R-250 for 30 min and then decolorized with 5% ethanol and 7.5% acetic acid. The gels were scanned, photographed, and analyzed using a gel imager (GS-900, BIO-RAD, USA). Bands were analyzed using Image J software.

2.8. Total Sulfhydryl Content

The total sulfhydryl groups of MPs were measured by a total sulfhydryl measurement kit (BC5805, Beijing Solepol Technology Co., Ltd.). The concentration of MPs solution was diluted to 5 mg/mL. According to the kit instructions, Tris-Gly buffer was added first and mixed thoroughly. Then, a certain amount of DTNB was added, mixed thoroughly, and the reaction was carried out while avoiding light at 4°C. After the reaction, centrifugation (3000 r/min, 10 min) was performed. The supernatant was taken and added to a 96-well plate, and the absorbance was measured at 412 nm using an enzyme meter (20M/*, Tecan Spark, Switzerland).

2.9. Carbonyl Content

The carbonyl content of MPs was measured using the Protein Carbonyl Content Kit (BC1275, Beijing Soleberg Technology Co., Ltd.). The concentration of MPs was diluted to 5 mg/mL and then mixed with 2,4-dinitrophenylhydrazine (DNPH). The reaction was performed at room temperature and avoided light for 1 h. Then, trichloroacetic acid was added, centrifuged at 12000 r/min, 4°C for 15 min, and the supernatant was discarded. After that, precipitation was washed and centrifuged 3 times (12000 r/min, 15 min, 4 °C) with a mixture of ethyl acetate: ethanol (1:1, v/v), dissolved in 6 mol/L guanidine hydrochloride solution, and water-bathed at 37°C. When the precipitation was completely dissolved, centrifugation was performed at 12000 r/min for 10 min, and supernatant was discarded. The absorbance was measured at 370 nm using an enzyme marker.

2.10. Secondary Structure

The secondary structure of MPs was detected by circular dichroism (Chirascan qCD, APL, UK) as described by Jia et al. [12] with slight modifications. MPs were diluted to 0.1 mg/mL. Then 1 mL of diluted MPs was taken for test. Spectra was acquired by scanning in the wavelength range of 200-260 nm. Contents of secondary structure were measured by CDNN software. The instrument scan rate was 100 nm/min.

 doi:10.20944/preprints202502.1353.v1

2.11. Preparation of MP Gels

MP gels were prepared as described by Shi, et al. [13] with slight modifications. Six equal MP solutions were adjusted to 50 mg/mL with the prepared 0, 5, 10, 15, 20, and 25 s PAW, respectively. Then 10 g of MPs were filled into a 10 mL beaker, sealed, placed in water bath and heated to 80°C for 30 min. After heating, samples were immediately cooled in ice bath for 10 minutes and placed in a 4°C refrigerator for 12 h to obtain the MP gels.

2.12. Color and Whiteness

The color and whiteness of MP gels was detected referring to the method of Wang et al. [14]. A fully automated colorimeter and a 10° field of view in 0/d mode was utilized to measure the color of gels. Before measurement, a standard color difference plate (standard values: L* = 94.81, a* = 100.00, b* = 107.32) was used to calibrate the colorimeter. After calibration, 6 random points were measured for each sample, and the L*, a*, b* and whiteness (W) of the MP gels were recorded. The average of the six measurements was taken. Gel whiteness was calculated following the formula below:

$$\textbf{Gel whiteness} = \mathbf{100} - \sqrt{（\mathbf{100} - \mathbf{L^*}）^{\mathbf{2}} + \mathbf{a^{*2}} + \mathbf{b^{*2}}} \quad (2)$$

2.13. Gel Strength

Gel strength was determined by a TA.XT. plus texture analyzer equipped with a cylindrical probe (P/0.5R) (TA.XT. plus, Stable Micro Systems, UK) referring to the method of Li, et al., (2019). The speed was set to 2.0 mm/s before and after the test, and 1.0 mm/s during the test. The trigger force was 5 g and the compression deformation was 50%. Each set of samples was measured six times.

2.14. Textural Properties

Textural properties including hardness, resilience, recoverability, adhesiveness, cohesiveness, and chewability of MP gels were tested as described by Li et al. [15]. with slightly modifications. MP gels were split into equally sized cylinders (2.0 cm thickness, 2.5 cm diameter). Texture analyzer equipped with a P/50 probe (TA.XT. plus, Stable Micro Systems, UK) was used and the speed before, during, and after the test was 2, 1, and 2 mm/s, respectively. And a double compression cycle test was performed with a compression percentage of 50% of the height of the sample.

2.15. Moisture Distribution

The internal moisture distribution of MP gels was detected by low-field nuclear magnetic resonance (LF-NMR) as described by Cheng et al. [16]. Samples (~ 2 g) were put in 2 mL cylindrical tubes and then scanned by LF-NMR analyzer (NM120, Niumag, China). The transverse relaxation times of the samples were recorded by Carr-Purcell-Meiboom-Gill (CMPG) sequence T2. Parameter settings as follows: sampling frequency was 200 KHz, the echo count was 15000, the time between 90° and 180° pulses was 13 us, the scanning range was 0 - 10000 ms, and there were 4 repetitions. Finally, samples were tested with the multi-spin echo pulse sequence imaging.

2.16. Secondary Structure

Fourier transform infrared spectroscopy (FTIR) (Vertex 70, Bruker, German) was used to analyzed the secondary structure of MPs in gels as described by Sun et al. [17]. Prepared gel samples were frozen by liquid nitrogen and then freeze-dried using a freeze dryer. Then KBr were mixed with dried gel samples in a ratio of 100:1 (w/w), ground into powder with a special mortar, and pressed into thin tablets by a tablet press for infrared determination. Measurement parameters were set as follows: scanning time: 32 s, resolution: 4 cm^{-1}, scanning range: 4000 - 400 cm^{-1}. The results of the scans were deconvoluted with Gaussian fitting using Peak fit 4.12 software to analyze the relative content of secondary structure of MP in gels.

 doi:10.20944/preprints202502.1353.v1

2.17. Molecular Forces

Molecular forces were detected according to the method of Xiong et al. [18]. with minor modifications. Two grams of the five prepared MP gel samples, weight 2 grams, were taken and added to 10 mL of the following reagents: S1: 0.05 mol/L NaCl, S2: 0.6 mol/L NaCl, S3: 0.6 mol/L NaCl + 1.5 mol/L Urea, S4: 0.6 mol/L NaCl + 8 mol/L Urea, and S5: 0.6 mol/L NaCl + 8 mol/L Urea + 0.5 mol/L β-mercaptoethanol, respectively. After that, sample was homogenized at 10000 r/min and allowed to stand at 4 °C for 1 h. After reaction, centrifugation was performed at 10000 g for 15 min. The supernatant was taken and the protein concentration was measured by bisulfite method. Molecular forces were calculated following the formula below:

Ionic bond content = S2 - S1.

Hydrogen bonding content = S3 - S2.

Hydrophobic interaction content = S4 - S3.

Disulfide bond content = S5 - S4.

2.18. Microstructure

High-resolution cold-field scanning electron microscopy (FE-SEM) (Regulus 8100, HITACHI, Japan) was used to observe the microstructure of MP gels according to the method of Zhou et al. [19]. Prepared MP gels were sliced into small pieces and placed in special sample trays for FE-SEM. Liquid nitrogen was used for rapid freezing of the samples. The samples were transported into the preparation chamber using the instrument's own transportation bar, and the surface of the samples was sliced by a special knife at very low temperatures. Sublimation was carried out at -75 °C for 15 min, followed by gold sputtering at 10 mA for 60 s. Then, sample was transported to the observation chamber. The microstructure of the MP gels was photographed under an accelerating voltage of 3 kV at magnifications of 1000× and 3000×, respectively.

2.19. Statistical Analysis

All experiments were carried out at least 3 times in parallel. Data were analyzed by one-way analysis of variance (ANOVA) with SPSS 25.0 software (SPSS 25.0 for windows, SPSS Inc, Chicago, IL, USA). Results of the experiment were presented as mean ± standard deviation. Figures were drawn using Origin 2023 (Origin Lab Co., Northampton, MA, USA). Significance was analyzed using Duncan's multiple comparison test ($P<0.05$).

3. Results and Discussion

3.1. Surface Hydrophobicity

BPB bound reflects surface hydrophobicity of protein, the higher BPB bound, the stronger the surface hydrophobicity of protein (Li et al., 2019). As presented in Figure 1(A), the surface hydrophobicity of MPs increased after PAW treatment. PAW obtained with the longer plasma treatment presented greater ability to enhance the surface hydrophobicity of MPs. Compared to control group, surface hydrophobicity was significantly higher in PAW15s, PAW20s, and PAW25s groups ($P<0.05$). A maximum value of 21.45 μg is observed in PAW25s group but showed insignificantly differences compared to PAW20s group ($P>0.05$). The large amounts of H_2O_2 and O_2 contained in PAW accelerate the oxidation of MPs to some extent, resulting in the more exposure of hydrophobic groups [20]. Previous study has shown that the gradual increase of ROS radicals and hydroxyl radicals in PAW would attack hydrophobic amino acids and further improve the surface hydrophobicity of proteins [21,22]. Furthermore, Li et al. [23] found that as PAW treatment time increased, the surface hydrophobicity of MPs increased accordingly, which is consistent with our results.

 doi:10.20944/preprints202502.1353.v1

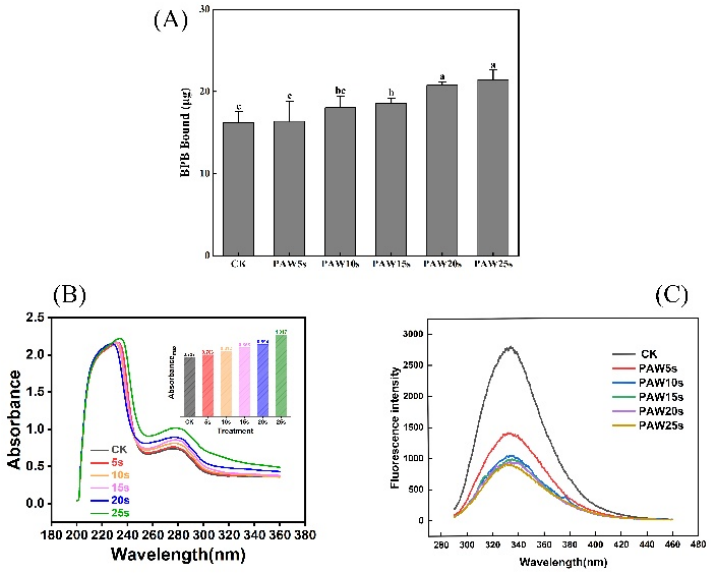

Figure 1. Effect of different PAW treatments on the surface hydrophobicity (A), ultraviolet absorption spectrum (B) and fluorescence spectrum (C) of MPs extracted from thawed pork. Different lowercase superscripts indicate significant differences (P<0.05). CK, control. PAW5s. PAW10s. PAW15s. PAW20s. PAW25s.

3.2. Ultraviolet Spectroscopy

Tryptophan (Trp) and tyrosine (Tyr) residues in proteins could absorb UV light and the absorption intensity usually used to reflect the changes in protein conformation. As shown in Figure 1(B), after PAW treatment, the UV absorption intensity of MP was significantly enhanced from 0.729 to 1.017 (P<0.05), which showed a positive correlation with the PAW treatment time. Besides, in PAW25s group, the maximum absorption wavelength turned to 278 nm, indicating that with the increased of PAW treatment time, more hydrophobic groups exposed and the polarity of amino acids switched at this time. In this case, the interactions between MPs enhanced and further promoted the aggregation of MPs [24]. Qian et al. [7] used PAW to treat MPs of chicken and found that the maximum absorption wavelength of MPs changed from 287 nm to 297 nm after PAW treatment, reflecting a significantly variation of the aromatic amino acid residues of MPs.

3.3. Intrinsic Fluorescence Spectroscopy

Fluorescence energy in microenvironment is extremely easy to induce the changes of intrinsic fluorescence of tryptophan and tyrosine residues in proteins. Changes in fluorescence intensity responds to the changes in protein tertiary structure [25]. As presented in Figure 1(C), PAW-treated MPs underwent a significant decrease of the fluorescence intensity (P<0.05) compared to control group. Besides, the fluorescence intensity continuously decreased with the prolongation of the PAW treatment time. Studies have verified lower fluorescence intensity accompanies by red-shifted fluorescence spectra indicates the deeper oxidation of protein [24]. In this study, MPs treated with PAW showed significantly lower fluorescence intensity, reflecting that PAW deepened the oxidation of MPs. This results also corresponds to the results of surface hydrophobicity of MPs. The decreased in fluorescence intensity caused by the oxidation of amino acid residues in MPs, resulting in the breakage of polypeptide chains and the formation of cross-linked protein aggregates. With fewer tyrosine and tryptophan residues exposed, the polarity to the fluorescence energy of the microenvironment attenuated [20].

3.4. SDS-PAGE

The aggregation and degradation of MPs after PAW treatments was determined by SDS-PAGE. As presented in Figure 2(A), there were two clearly visible bands at 45 kDa and 200 kDa correspond

 doi:10.20944/preprints202502.1353.v1

to actin and myosin heavy chain, respectively. In addition, bands of myosin light chains (16-25 kDa), troponin (35 kDa), and troponin T (38 kDa) were also detected. The intensity of myosin heavy chains in reductive SDS-PAGE was analyzed by Image J software and presented in Figure 2(B). The results showed that, the composition of MPs remained unchanged after PAW treatments, but in the non-reducing condition, bands intensity of PAW25s group weakened. This was likely due to the aggregates formation in PAW25s group, possibly as a result of the interactions formation between the carbon-carbon covalent bonds of MPs induced by protein oxidation [26]. In a non-reduced environment, with the increasing time of PAW treatment, a clearly upward trend of bands intensities in the range of 180 kDa to 245 kDa was found. DTT as a kind of redox reagent could completely or partially disrupt disulfide bonds in proteins, thereby affecting protein structure and functions [27]. The bands intensity with molecular weight more than 245 kDa became lighter after the addition of DTT, demonstrating that more protein aggregates cross-linked by disulfide bonds were degraded. Xiong et al. [28] found that the addition of reductive agent (β-mercaptoethanol) to MPs solutions contained with H_2O_2 resulted in the darkening intensity of MHC bands. And the intensity darkened as the amount of H_2O_2 increased due to the ability of H_2O_2 to promote the disulfide formation between proteins. Therefore, in this study, PAW also promoted cross-linking of MPs through disulfide bonds, and the higher degree of MPs aggregation after PAW treatment may attribute to the lower degree of protein degradation.

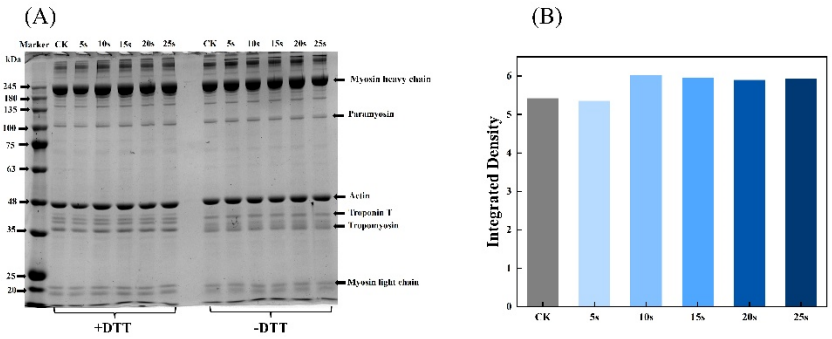

Figure 2. Effect of PAW treatments on SDS-PAGE (A) and relative band intensity (B) of MPs extracted from thawed pork. Different lowercase superscripts indicate significant differences (P<0.05). CK, control.

3.5. Total Sulfhydryl Content

Sulfhydryl groups (SH) contained in MP are highly sensitive to oxidation and then turn into disulfide bonds (S-S) [29]. Reduction of SH content represents that the SH group of cysteine is oxidized and the S-S increased. As shown in Figure 3(A), the total sulfhydryl content of MPs decreased significantly after PAW treatment (P<0.05), and reached a minimum value of 43.03 μmol/g-pro in PAW25s group. However, expect for PAW25s, the total sulfhydryl content showed insignificantly differences between other PAW groups (P>0.05). Cao et al. [25] investigated the oxidation of MPs and found that the SH group in actin was sensitive to hydroxyl radicals and was easily converted to intermolecular S-S after oxidation. Besides, Fe^{3+} catalyzes the generation of hydroxyl radicals from H_2O_2, and to some extent, Fe^{3+}-induced oxidation has a synergistic effect with PAW.

 doi:10.20944/preprints202502.1353.v1

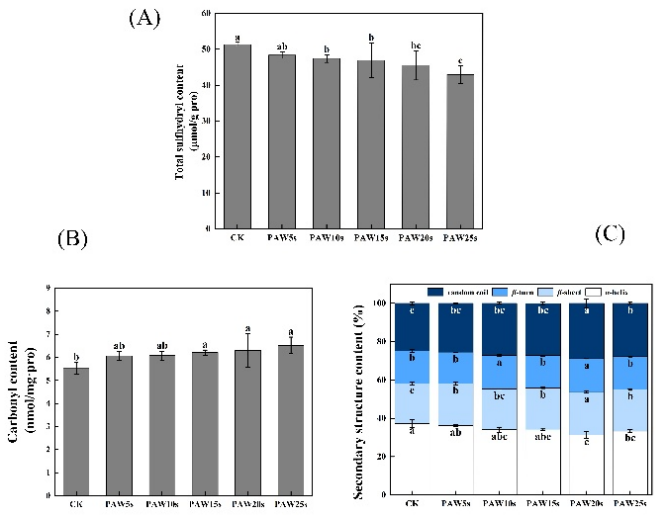

Figure 3. Effect of PAW treatments on total sulfhydryl content (A), carbonyl content (B) and secondary structure (C) of MPs extracted from thawed pork. Different lowercase superscripts indicate significant differences (P<0.05). CK, control.

3.6. Carbonyl Content

Carbonyl groups are the mainly oxidation products of tryptophan, proline, arginine, and lysine residues in proteins. Proteins with -NH and -NH_2 groups in side chains are easily deamidated to form carbonyl derivatives [30]. As shown in Figure 3(B). The carbonyl content was 5.77 nmol/mg pro in control group. Compared to control group, carbonyl content in PAW15s, 20s and 25s groups significantly increased (P<0.05) and reached a maximum value of 6.52 nmol/mg pro in PAW25s group. PAW5s and PAW10s group had higher carbonyl content than control group but showed insignificantly differences (P>0.05). The results indicated that the oxidation degree of MPs was not significant influenced by short time (5 s, 10 s) PAW treatment, but was further improved with the prolonged treatment time. The impact of energetic particles in the PAW solution also disrupts the structure of MPs, causing more residues of MPs expose and further promoting the carbonylation of protein residues [31]. PAW treatment to some extent improved the oxidation of MPs, which was corresponded to the previously results of total sulfhydryl content of MPs.

3.7. Secondary Structure

Figure 3(C) shows the changes in the secondary structure of MP. After PAW treatment, the α-helix, β-turn, β-sheet and random coil content of MP changed perceptibly. Among them, the α-helix content generally presented a decreasing trend and reached the minimum value of 31.25% in PAW20s group, which was significantly lower than that in other groups (P<0.05). The β-sheet and random coil content gradually increased accompanied by the treatment time of PAW increased to 20s, and then decreased at 25s treatment time. But compared to control group, random coil and β-sheet content in PAW25s group was significantly higher (P<0.05). PAW5s, PAW15s, and PAW25s groups presented insignificantly differences of β-turn content compared with control group (P>0.05), while β-turn content in PAW10s and PAW20s groups was significantly higher than that in control group (P<0.05). Usually, proteins maintain their biologically active structures in vitro through weak interactions such as hydrophobic interactions, hydrogen bonding, and ionic bonding. When the surroundings change, these interactions may be altered, leading to protein denaturation and inactivation. Hydrogen bonds formed between the amino hydrogen (NH-) and carbonyl oxygen (-CO) in the peptide chain help stabilize the α-helix structure [32]. PAW contains a large number of active substances such as NO_3^-, NO^-, and RONS. These substances could weaken the interaction between proteins and water, break hydrogen bonds, and promote the α-helix structure to deconvolute and transform into other structures [33]. Therefore, the further prolonged of the PAW treatment time decreased the α-helix

 doi:10.20944/preprints202502.1353.v1

content in this study. A certain degree of PAW treatment decreased the α-helix content of protein, resulting in more exposure of hydrophobic groups, more aggregation of proteins, and more tightly linked between proteins [34], which was corresponded to the previously results of surface hydrophobicity of MPs.

3.8. Color and Whiteness of MP Gels

Color is a very important sensory indicator for meat products and gels. As presented in Table 1, with the increased PAW treatment time, L*, a*, b*, and whiteness showed a trend of first increasing and then decreasing. All of these indexes reached the maximum value in PAW20s group. The whiteness of the gels improved from the initial 76.35 to 85.06. Usually, the whiteness value of gel is closely related to gel quality [35]. PAW treated groups presented significantly higher whiteness than control group (P<0.05), demonstrating that gels prepared by PAW treated MPs might contains higher content of moisture, which enhances the light reflection of gels. PAW treatment may help increase the water content in network structure of MP gels.

Table 1. Effect of PAW on the color and whiteness of MP gels.

	L^*	a^*	b^*	W
CK	76.75±1.26^{d}	-2.45±0.17^{c}	-3.52±0.64^{c}	76.35±1.32^{d}
PAW5s	80.32±0.38^{c}	-2.38±0.02^{c}	-2.59±0.05^{abc}	80.01±0.36^{c}
PAW10s	81.47±0.53^{c}	-1.87±0.11^{b}	-3.32±0.48^{bc}	81.08±0.43^{c}
PAW15s	83.03±0.36^{b}	-1.83±0.04^{b}	-2.54±0.44^{abc}	82.74±0.32^{b}
PAW20s	85.28±0.63^{a}	-1.59±0.02^{a}	-1.89±0.41^{a}	85.06±0.59^{a}
PAW25s	83.11±0.79^{b}	-2.04±0.14^{b}	-2.38±0.81^{ab}	82.82±0.85^{b}

Note: Different letters for the same indicator represent significant differences (P<0.05).

3.9. Gel Strength

The strength of MP gels is presented in Figure 4(A). The gradually increase of gel strength was observed with the increase of PAW treatment time. The control group had the smallest gel strength of 88.645 g (P<0.05). And compared to control group, MP gels in the PAW treatment groups significantly increased (P<0.05) and reached a maximum value of 120.07 g in PAW25s group. Study has proven that, the adequate oxidative stress induced by reactive oxygen species in PAW increases the intramolecular and intermolecular interactions of MPs, contributing to the improvement of MP gel strength [36]. It is consistent with our results. A significant improvement of MP gel strength was observed after MPs treating with PAW, indicating a positively role of PAW in the improvement of MP gel quality.

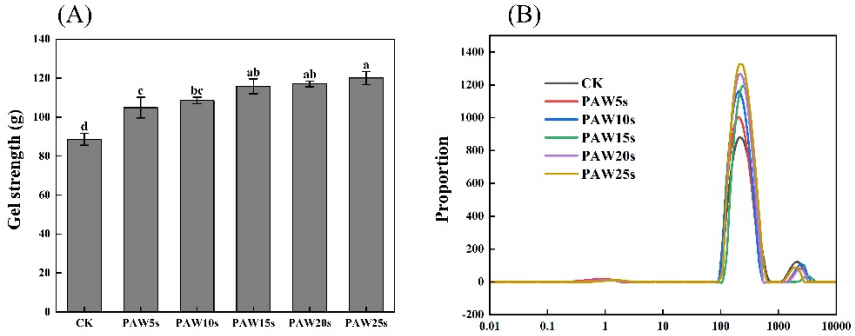

Figure 4. Effect of PAW treatments on gel strength (A) and moisture distribution (B) of MP gels. Different lowercase superscripts indicate significant differences (P<0.05). CK, control.

3.10. Moisture Distribution

 doi:10.20944/preprints202502.1353.v1

As a non-destructive method, LF-NMR has been widely used to evaluate the distribution and migration of water in protein gels [37]. Three types of water reflected by three characteristic peaks, respectively: T_{2b} (0.1-10 ms, bound water firmly bonds to the protein gel), T_{21} (10-1000 ms, immobilized water limited by the structure of the protein gel), and T_{22} (1000-10000 ms, free water located outside the protein gel). The results in this study are in accordance with the relaxation time of meat gels as described by Wang et al. [38] and Zhang et al. [39]. As shown in Figure 4(B), there was insignificantly difference of T_{2b} relaxation time among all groups (P>0.05), but a significantly change in the relaxation time of T_{21} and a significantly increase in the peak amplitude of T_{21} in PAW groups was observed compared to control group (P<0.05). Wang et al. [3] found that the mobility of water is strongly related to the relaxation time, reflecting the binding of water to macromolecules. Therefore, the results of our study demonstrate that PAW treatment promoted the interception of more free water and improved the water retention of the gels. PAW might enhance the intermolecular forces between MPs and promote the formation of gels with homogeneous and tight network structures. However, the differences in the proportion of peak area between different PAW groups were insignificant (P>0.05). This may due to the short treatment time of the PAW. The relaxation time of T_{22} in PAW groups was significantly lower than that in control group (P<0.05), also illustrating that gels in PAW groups had less content of free water and higher water-holding capacity. The peak area ratios of T_{22}, T_{21}, and T_{2b} were displayed as P_{22}, P_{21}, and P_{2b}, respectively, and presented in Table 2. As shown in Table 2, there was no significantly difference (P>0.05) between the P_{2b} of each group, demonstrating that the bound water in gels was unaffected by PAW treatment. However, compared with control group, P_{21} and P_{22} in PAW groups was significant increased and significant decreased (P<0.05), respectively. In MP gels, the content of immobilized water increased significantly and the content of free water decreased significantly after MPs treating with PAW. Differences of P_{21} and P_{22} were insignificant between different PAW groups, which might due to the short duration of PAW treatment and was corresponded to the results of T_{2b}, T_{21}, and T_{22}.

Table 2. Effect of PAW on moisture distribution of MP gels.

	T_{2b}	T_{21}	T_{22}
CK	0.825±0.195^{a}	92.573±0.229^{b}	6.662±0.128^{a}
PAW5s	0.867±0.783^{a}	94.798±0.310^{a}	4.335±0.493^{b}
PAW10s	0.700±0.056^{a}	96.287±0.173^{a}	3.014±0.115^{b}
PAW15s	0.797±0.128^{a}	96.815±0.130^{a}	2.389±0.009^{b}
PAW20s	0.698±0.142^{a}	95.965±0.231^{a}	3.336±0.368^{b}
PAW`25s	0.749±0.147^{a}	95.362±2.428^{a}	3.889±2.459^{b}

Note: Different letters for the same indicator represent significant differences (P<0.05).

3.11. Textural Properties

Figure 5 presents the textural properties of MP gels. As shown in Figure 5, the hardness, chewiness, and adhesiveness of gels were significantly higher in PAW groups compared to control group (P<0.05). But the resilience and cohesiveness of gels presented insignificantly differences between all groups (P>0.05). PAW improves the solubility of MPs before heating, which provides more opportunities for adequate interactions between proteins, and further contributes to the formation of protein gels with higher textural properties [40]. Furthermore, Luo et al. [41] found that plasma could promote the emulsification properties of MPs, which was closely positive related to the gel properties of MPs.

 doi:10.20944/preprints202502.1353.v1

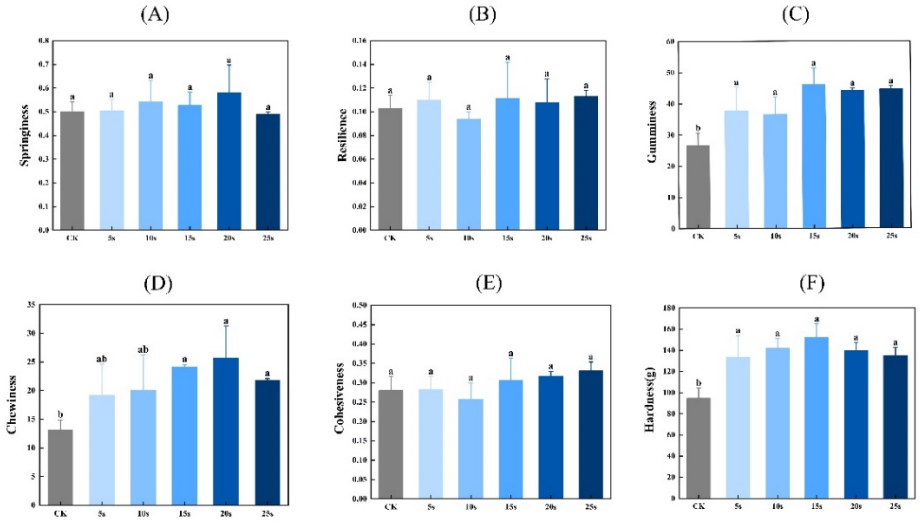

Figure 5. Effect of PAW treatments on the textural properties of MP gels. A-F, Springiness (A), Resilience (B), Gumminess (C), Chewiness (D), Cohesiveness (E), Hardness (F). Different lowercase superscripts indicate significant differences (P<0.05). CK, control.

3.12. FTIR

The secondary structure of MP in gels are determined by Fourier infrared spectroscopy (FTIR). Figure 6(A) shows the FTIR spectra in the range of 400 - 4000 cm^{-1}. The amide I band (1600 - 1700 cm^{-1}) is a typical absorption peak, which is mainly caused by C=O stretching vibration, N-H bending vibration and C-N stretching vibration, and is often used to characterize secondary structure changes of MP in gels. Absorption peaks correspond to secondary structure of protein as follows: β-sheet 1600 to 1640 cm^{-1}, random coil 1640 to 1650 cm^{-1}, α-helix 1650 to 1660 cm^{-1}, β-turn 1660 to 1700 cm^{-1} [42]. Figure 6(B) presents the α-helix, β-turn, β-sheet and random coil content of the MPs in gels. Expect for PAW5s group, the α-helix content in other PAW groups was significantly lower compared to control group (P<0.05), and reached a minimum in PAW20s group. The β-sheet content in PAW groups, expect for PAW25s, was significantly higher compared to control group (P<0.05). However, there were insignificant differences of β-turning content between all groups (P>0.05). It is generally recognized that during the thermal induction of proteins into gels process, α-helix are converted to β-turn and β-sheet, and a higher β-sheet content represents a better secondary structure of proteins in gels [43]. Furthermore, the ROS, hydroxyl radicals, and other reactive substances contain in PAW help increase the conversion of α-helix during the formation of thermal induced MP gels [44]. Therefore, the results of this study confirm and indicate that the previously PAW treatment of MPs promoted the conversion from α-helix to β-sheet of MPs during the formation of thermal induced gels.

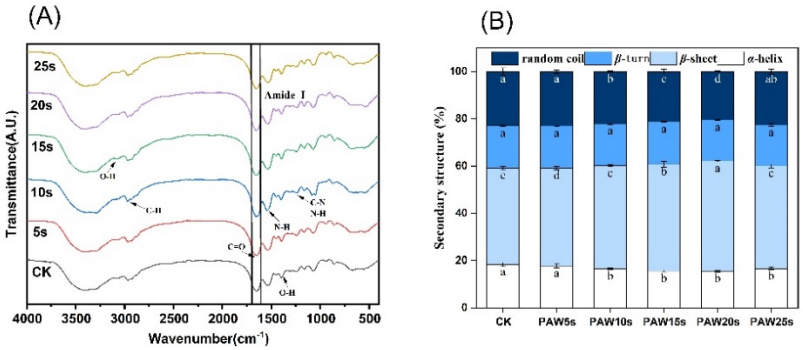

Figure 6. Effect of PAW treatments on secondary structure of MP in gels. A-B, FTIR spectra (A), secondary structure content (B). Different lowercase superscripts indicate significant differences (P<0.05). CK, control.

 doi:10.20944/preprints202502.1353.v1

3.13. Molecular Forces

The detection of intermolecular forces in MP gels provides insight into the interactions between molecules occurs in MP gels [45]. As presented in Figure 7, as the treatment time increase, the ionic bonding content of PAW groups significantly increased (P<0.05) compared to control group, reaching the maximum value of 49.11% in PAW25s group. Hydrogen bonding content decreased significantly in PAW groups compared with control group (P<0.05), reaching the minimum in PAW25s group, with a reduction of 29.68%, indicating that PAW significantly enhanced the breakage of hydrogen bonds. The hydrophobic interactions showed a significant increase of 48.11% with the extension of PAW treatment time (P<0.05). And the disulfide bonds of gels significantly increased (P<0.05) by 43.72% after PAW treatment. The enhanced oxidation of MPs after PAW treatment promotes sulfhydryl groups in MPs to form more disulfide bonds during gel formation, leading to the obviously increase of the disulfide bonds content in all PAW treatments. Hydrophobic interactions play an important role in the formation of gels and the disulfide bonds closely relates to the three-dimensional structure of proteins in gels [46]. Thus, the results of this study demonstrates that the application of PAW was beneficial to the formation of gels with stable structures, contributing to the enhancement of gel properties of MPs.

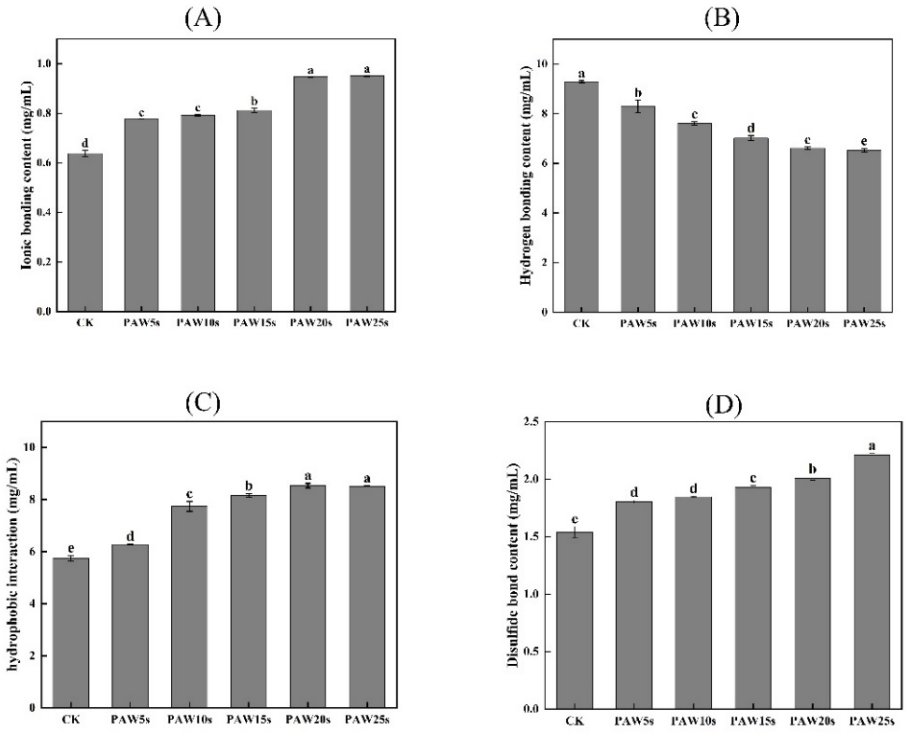

Figure 7. Effect of PAW treatments on molecular forces in MP gels. A-C, Ionic bonding content (A), Hydrogen bonding content (B), Hydrophobic interaction (C), Disulfide bond content (D). Different lowercase superscripts indicate significant differences (P<0.05). CK, control.

3.14. Microstructure

The observation of the microstructure of MP gels was performed by high-resolution cold-field scanning electron microscopy (FE-SEM) and presented in Figure 8. As shown in Figure 8, the MP gels in all groups showed macroscopically homogeneous structures as the typical carnosine gels. Compared to control group, the microstructure of PAW-treated MP gels was denser and more homogeneous. MPs treated with PAW undergone more oxidative denaturation, resulting in more exposure of sulfhydryl groups and hydrophobic groups of MPs. Furthermore, the heat-induced gelation results in the cross-linking of exposed hydrophobic groups and the formation of disulfide bonds through sulfhydryl groups [47]. Therefore, the stronger protein interactions in PAW-treated gels contribute to the formation of gels with homogeneous microstructures and stronger texture

 doi:10.20944/preprints202502.1353.v1

properties. In other words, PAW treatment dispersed the protein aggregates, enhanced protein-water interactions, and finally formatted denser gels. Particularly, MP gels of PAW20s and PAW25s groups presented the best microstructures.

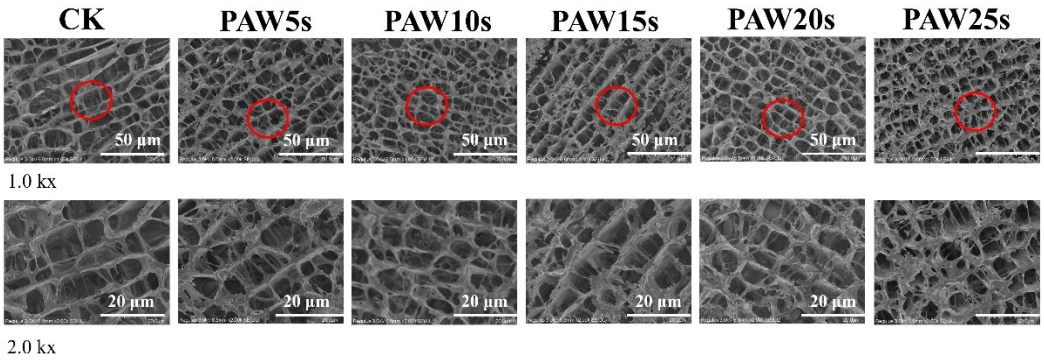

Figure 8. Effect of PAW treatments on the microstructure of MP gels. CK, control.

4. Conclusions

PAW treatment promoted the partial oxidation of MPs and generated more disulfide bonds in MPs. The changes of amino acid polarity and the exposure of hydrophobic groups in PAW-treated MPs also promoted intra-protein and protein-protein interactions. The enhanced properties of PAW-treated MPs of thawed pork promoted to the formation of MP gels with more stable and densely structures. In particular, PAW treatment for 20 s significantly improved the strength, textural properties, water-holding capacity and water distribution of the MP gels. To sum up, PAW treatment altered the intermolecular forces and the structures of MPs extracted from thawed pork and helped improve the gel properties of MPs extracted from thawed pork significantly. This study develops a new method to fix and improve the processing functions of MPs of thawed meat, and may contributes to reduce wastage of thawed meat products.

Author Contributions: M. D.: Conceptualization, Data curation, Investigation, Funding acquisition, Formal analysis, Roles/Writing-original draft, Writing-Review & editing; F. H.: Formal analysis, Investigation, Data curation, Roles/Writing-original draft; S. S.: Data curation, Formal analysis, Writing-Review & editing; K. L.: Conceptualization, Funding acquisition, Supervision, Writing-Review & editing; Q. X.: Conceptualization, Funding acquisition; J. L.: Writing-Review & editing; L. C.: Writing-Review & editing; Y. B.: Conceptualization, Supervision, Funding acquisition, Writing-Review & editing. All authors have read and agreed to the published version of the manuscript.

Funding: This research was supported by National Natural Science Foundation of China (32372382) in China; School-Enterprise Research and Development Center Project of Henan Province (25CY040) in China.

Institutional Review Board Statement: This statement was excluded because the study did not require ethical approval.

Informed Consent Statement: Informed consent was obtained from all subjects involved in the study.

Data Availability Statement: The data that support the results of this study are available on re-quest from the corresponding author.

Conflicts of Interest: The authors declare that they have no known competing financial interests or personal relationships that could have appeared to influence the work reported in this paper.

 doi:10.20944/preprints202502.1353.v1

References

1. Medic H.; Djurkin Kusec I.; Pleadin J; Kozacinski, L.; Njari, B.; Hengl, B.; Kusec, G. The Impact of Frozen Storage Duration on Physical, Chemical and Microbiological Properties of Pork. Meat Science, 2018, 140, 119-127.
2. Kim H. W.; Kim J. H.; Seo J. K.; Setyabrata, D.; Kim, Y. H. B. Effects of Aging/freezing Sequence and Freezing Rate on Meat Quality and Oxidative Stability of Pork Loins. Meat Science, 2018, 139, 162-170. https://doi.org/10.1016/j.meatsci.2018.01.024
3. Wang, Y.; Bai, Y. H.; Ma, F.; Li, K.; Zhou, H.; Chen, C. G. (2021). Combination Treatment of High-pressure and CaCl2 for the Reduction of Sodium Content in Chicken Meat Batters: Effects on Physicochemical Properties and Sensory Characteristics. International Journal of Food Science and Technology, 2021, 56(12), 6322-6334. https://10.1111/ijfs.15346
4. Chaijan, M.; Chaijan, S.; Panya, A.; Nisoa, M.; Cheong, L. Z.; Panpipat, W. High Hydrogen Peroxide Concentration-low Exposure Time of Plasma-activated Water (PAW): A Novel Approach for Shelf-life Extension of Asian Sea Bass (Lates calcarifer) Steak. Innovative Food Science & Emerging Technologies, 2021, 74, 102861. https://doi.org/10.1016/j.ifset.2021.102861
5. Laurita, R.; Gozzi, G.; Tappi, S.; Capelli, F.; Bisag, A.; Laghi, G.; Gherardi, M.; Cellini, B.; Abouelenein, D.; Vittori, S. Effect of plasma activated water (PAW) on rocket leaves decontamination and nutritional value. Innovative Food Science & Emerging Technologies, 2021, 73, 102805. https://doi.org/10.1016/j.ifset.2021.102805
6. Li, M. Z.; Wang, X.; Shi, T.; Xiong, Z. Y.; Jin, W. A.; Bao, L.; Monto, A. R.; Yuan, L.; Gao, R. C. Mechanism of Plasma-activated Water Promoting the Heat-induced Aggregation of Myofibrillar Protein from Silver Carp (Aristichthys Nobilis). Innovative Food Science & Emerging Technologies, 2024, 91, 103555. https://doi.org/10.1016/j.ifset.2023.103555
7. Qian, J.; Wang, Y. Y.; Zhuang, H.; Yan, W. J.; Zhang, J. H.; Luo, J. Plasma Activated Water-induced Formation of Compact Chicken Myofibrillar Protein Gel Structures with Intrinsically Antibacterial Activity. Food Chemistry, 2021, 351, 129278. https://10.1016/j.foodchem.2021.129278
8. Liao, X. Y.; Liu, D. H.; Xiang, Q. S.; Ahn, J.; Chen, S. G.; Ye, X. Q.; Ding, T. Inactivation Mechanisms of Non-thermal Plasma on Microbes: A Review. Food Control, 2017, 75, 83-91. https://doi.org/10.1016/j.foodcont.2016.12.021
9. Zhu, M. M.; Xing, Y.; Zhang, J.; Li, H. J.; Kang, Z. L.; Ma, H. J.; Zhao, S. M.; Jiao, L. X. Low-frequency Alternating Magnetic Field Thawing of Frozen Pork Meat: Effects of Intensity on Quality Properties and Microstructure of Meat and Structure of Myofibrillar Proteins. Meat Science, 2023, 204, 109241. https://doi.org/10.1016/j.meatsci.2023.109241
10. Li, F. F.; Wang, B.; Liu, Q.; Chen, Q.; Zhang, H. W.; Xia, X. F.; Kong, B. H. Changes in Myofibrillar Protein Gel Quality of Porcine Longissimus Muscle Induced by Its Stuctural Modification under Different Thawing Methods. Meat Science, 2019, 147, 108-115. https://10.1016/j.meatsci.2018.09.003
11. Liu, J.; Arner, A.; Puolanne, E.; Ertbjerg, P. On the Water-holding of Myofibrils: Effect of Sarcoplasmic Protein Denaturation. Meat Science, 2016, 119, 32-40. https://doi.org/10.1016/j.meatsci.2016.04.020
12. Jia, G. L.; Nirasawa, S.; Ji, X. H.; Luo, Y. K.; Liu, H. J. Physicochemical Changes in Myofibrillar Proteins Extracted from Pork Tenderloin Thawed by A High-voltage Electrostatic Field. Food Chemistry, 2018, 240, 910-916. https://doi.org/10.1016/j.foodchem.2017.07.138
13. Shi, T.; Xiong, Z. Y.; Jin, W. G.; Yuan, L.; Sun, Q. C.; Zhang, Y. H.; Li, X. T.; Gao, R. C. Suppression Mechanism of l-Arginine in the Heat-induced Aggregation of Bighead Carp (Aristichthys nobilis) Myosin: The Significance of Ionic Linkage Effects and Hydrogen Bond Effects. Food Hydrocolloids, 2020, 102, 105596. https://doi.org/10.1016/j.foodhyd.2019.105596
14. Wang, Y.; Yuan, J. J.; Li, K.; Chen, X.; Wang, Y. T.; Bai, Y. H. Evaluation of Chickpea Protein Isolate as A Partial Replacement for Phosphate in Pork Meat Batters: Techno-functional Properties and Molecular Characteristic Modifications. Food Chemistry, 2023 404, 134585. https://doi.org/10.1016/j.foodchem.2022.134585

 doi:10.20944/preprints202502.1353.v1

15. Li, K.; Wang, L. M.; Gao, H. J.; Du, M. T.; Bai, Y. H. Use of Basic Amino Acids to Improve Gel Properties of PSE-like Chicken Meat Proteins Isolated Via Ultrasound-assisted Alkaline Extraction. Journal of Food Science, 2023, 88(12), 5136-5148. https://10.1111/1750-3841.16800
16. Cheng, S. S.; Wang, X. H.; Yang, H. M.; Lin, R.; Wang, H. T.; Tan, M. Q. Characterization of Moisture Migration of Beef During Refrigeration Storage by Low-field NMR and Its Relationship to Beef Quality. Journal of the Science of Food and Agriculture, 2020, 100(5), 1940-1948. https://10.1002/jsfa.10206
17. Sun, W. Z.; Zhou, F. B.; Sun, D. W.; Zhao, M. M. Effect of Oxidation on the Emulsifying Properties of Myofibrillar Proteins. Food and Bioprocess Technology, 2013, 6(7), 1703-1712. https://10.1007/s11947-012-0823-8
18. Xiong, Z. Y.; Shi, T.; Zhang, W.; Kong, Y. F.; Yuan, L.; Gao, R. C. Improvement of Gel Properties of Low Salt Surimi using Low-dose L-arginine Combined with Oxidized Caffeic Acid. Lwt-Food Science and Technology, 2021, 145, 111303. https://10.1016/j.lwt.2021.111303
19. Zhou, F. B.; Zhao, M. M.; Su, G. W.; Cui, C.; Sun, W. Z. Gelation of Salted Myofibrillar Protein under Malondialdehyde-induced Oxidative Stress. Food Hydrocolloids, 2014, 40, 153-162. https://10.1016/j.foodhyd.2014.03.001
20. Jiang, S. Q.; Yang, C. J.; Bai, R.; Li, Z. W.; Zhang, L. L.; Chen, Y.; Ye, X.; Wang, S. Y.; Jiang, H.; Ding, W. Modifying Duck Myofibrillar Proteins Using Sodium Bicarbonate Under Cold Plasma Treatment: Impact on the Conformation, Emulsification, and Rheological Properties. Food Hydrocolloids, 2024, 150 109682. https://10.1016/j.foodhyd.2023.109682
21. Inbakumar, S. (2010). Effect of Plasma Treatment on Surface of Protein Fabrics. In Journal of Physics: Conference Series, 2010, 208, 012111: IOP Publishing. DOI 10.1088/1742-6596/208/1/012111
22. Li, J.; Xiang, Q.; Liu, X.; Ding, T.; Zhang, X.; Zhai, Y.; Bai, Y. Inactivation of Soybean Trypsin Inhibitor by Dielectric-barrier Discharge (DBD) Plasma. Food chemistry, 2017, 232, 515-522. https://doi.org/10.1016/j.foodchem.2017.03.167
23. Li, M. Z.; Wang, X.; Shi, T.; Xiong, Z. Y.; Jin, W. A.; Bao, Y. L.; Monto, A. R.; Yuan, L.; Gao, R. C. (2024). Mechanism of Plasma-activated Water Promoting the Heat-induced Aggregation of Myofibrillar Protein from Silver Carp (Aristichthys Nobilis). Innovative Food Science & Emerging Technologies, 2024, 91, 103555. https://10.1016/j.ifset.2023.103555
24. Bußler, S.; Rumpold, B. A.; Fröhling, A.; Jander, E.; Rawel, H. M.; Schlüter, O. K. Cold Atmospheric Pressure Plasma Processing of Insect Flour from Tenebrio Molitor: Impact on Microbial Load and Quality Attributes in Comparison to Dry Heat Treatment. Innovative Food Science & Emerging Technologies, 2016, 36, 277-286. https://doi.org/10.1016/j.ifset.2016.07.002
25. Cao, Y.; True, A. D.; Chen, J.; Xiong, Y. L. Dual Role (Anti-and Pro-oxidant) of Gallic Acid in Mediating Myofibrillar Protein Gelation and Gel in Vitro Digestion. Journal of Agricultural and Food Chemistry, 2016, 64(15), 3054-3061. https://doi.org/10.1021/acs.jafc.6b00314
26. Nyaisaba, B. M.; Miao, W. H.; Hatab, S.; Siloam, A.; Chen, M. L.; Deng, S. G. Effects of Cold Atmospheric Plasma on Squid Proteases and Gel Properties of Protein Concentrate from Squid (Argentinus ilex) Mantle. Food Chemistry, 2019, 291, 68-76. https://10.1016/j.foodchem.2019.04.012
27. Chen, C. C.; Kao, M. C.; Chen, C. J.; Jao, C. H.; Hsieh, J. F. Improvement of Enzymatic Cross-linkin of Ovalbumin and Ovotransferrin Induced by Transglutaminase with Heat and Reducing Agent Pretreatment. Food Chemistry, 2023, 409, 135281. https://10.1016/j.foodchem.2022.135281
28. Xiong, G. Q.; Cheng, W.; Ye, L. X.; Du, X.; Zhou, M.; Lin, R. T.; Geng, S. R.; Chen, M. L.; Corke, H.; Cai, Y. Z. Effects of Konjac Glucomannan on Physicochemical Properties of Myofibrillar Protein and Surimi Gels from Grass Carp (Ctenopharyngodon idella). Food Chemistry, 2009, 116(2), 413-418. https://10.1016/j.foodchem.2009.02.056
29. Cui, C.; Zhou, X. S.; Zhao, M. M.; Yang, B. Effect of Thermal Treatment on the Enzymatic Hydrolysis of Chicken Proteins. Innovative Food Science & Emerging Technologies, 2009, 10(1), 37-41. https://10.1016/j.ifset.2008.09.003
30. Xia, T. L.; Xu, Y. J.; Zhang, Y. L.; Xu, L. A.; Kong, Y. W.; Song, S. X.; Huang, M. Y.; Bai, Y.; Luan, Y.; Han, M. Y.; Zhou, G. H.; Xu, X. L. Effect of Oxidation on the Process of Thermal Gelation of Chicken Breast Myofibrillar Protein. Food Chemistry, 2022, 384. https://10.1016/j.foodchem.2022.132368

 doi:10.20944/preprints202502.1353.v1

31. Estévez, M. Protein Carbonyls in Meat Systems: A Review. Meat science, 2011, 89(3), 259-279. https://10.1016/j.meatsci.2011.04.025
32. Liu, R.; Zhao, S. M.; Xiong, S. B.; Die, B. J.; Qin, L. H. Role of Secondary Structures in the Gelation of Porcine Myosin at Different pH Values. Meat science, 2008, 80(3), 632-639. https://10.1016/j.meatsci.2008.02.014
33. Bellissent-Funel, M. C.; Hassanali, A.; Havenith, M.; Henchman, R.; Pohl, P.; Sterpone, F.; van der Spoel, D.; Xu, Y.; Garcia, A. E. Water Determines the Structure and Dynamics of Proteins. Chemical Reviews, 2016, 116(13), 7673-7697. https://10.1021/acs.chemrev.5b00664
34. Yang, R.; Liu, Y.; Meng, D.; Wang, D.; Blanchard, C. L.; Zhou, Z. Effect of Atmospheric Cold Plasma on Structure, Activity, and Reversible Assembly of the Phytoferritin. Food Chemistry, 2018, 264, 264, 41-48. https://doi.org/10.1016/j.foodchem.2018.04.049
35. Zou, Q.; Liu, Y. D.; Luo, L. H.; Chen, Y. Y.; Zheng, Y. H.; Ran, G. L.; Liu, D. Y. Screening of Optimal Konjac Glucomannan-Protein Composite Gel Formulations to Mimic the Texture and Appearance of Tripe. Gels, 2024, 10(8), 528. https://10.3390/gels10080528
36. Zheng, J. B.; Han, Y. R.; Ge, G.; Zhao, M. M.; Sun, W. Z. Partial substitution of NaCl with Chloride Salt Mixtures: Impact on Oxidative Characteristics of Meat Myofibrillar Protein and Their Rheological Properties. Food Hydrocolloids, 2019, 96, 36-42. https://10.1016/j.foodhyd.2019.05.003
37. Wei, H. Y.; Luo, K. X.; Fu, R. H.; Lin, X. D.; Feng, A. G. Impact of the Magnetic Field-assisted Freezing on the Moisture Content, Water Migration Degree, Microstructure, Fractal Dimension, and the Quality of the Frozen Tilapia. Food Science & Nutrition, 2022, 10(1), 122-132. https://10.1002/fsn3.2653
38. Wang, L.; Zhang, M.; Bhandari, B.; Gao, Z. X. Effects of Malondialdehyde-induced Protein Modification on Water Functionality and Physicochemical State of Fish Myofibrillar Protein Gel. Food Research International, 2016, 86, 131-139. https://10.1016/j.foodres.2016.06.007
39. Zhang, Z. Y.; Regenstein, J. M.; Zhou, P.; Yang, Y. L. Effects of High Intensity Ultrasound Modification on Physicochemical Property and Water in Myofibrillar Protein Gel. Ultrasonics Sonochemistry, 2017, 34, 960-967. https://10.1016/j.ultsonch.2016.08.008
40. Chen, J. Y.; Ren, Y. X.; Zhang, K. S.; Xiong, Y. L. L.; Wang, Q.; Shang, K.; Zhang, D. Site-specific Incorporation of Sodium Tripolyphosphate into Myofibrillar Protein from Mantis Shrimp (Oratosquilla oratoria) Promotes Protein Crosslinking and Gel Network Formation. Food Chemistry, 2020, 312, 126113. https://10.1016/j.foodchem.2019.126113
41. Luo, J.; Xu, W. M.; Liu, Q.; Zou, Y.; Wang, D. Y.; Zhang, J. H. Dielectric Barrier Discharge Cold Plasma Treatment of Pork Loin: Effects on Muscle Physicochemical Properties and Emulsifying Properties of Pork Myofibrillar Protein. Lwt-Food Science and Technology, 2022, 162, 113484. https://10.1016/j.lwt.2022.113484
42. Cai, S.; Singh, B. R. Identification of Beta-turn and Random Coil Amide III Infrared Bands for Secondary Structure Estimation of Proteins. Biophysical Chemistry, 1999, 80(1), 7-20. https://10.1016/s0301-4622(99)00060-5
43. Jiang, Q.; Zhang, M.; Mujumdar, A. S.; Chen, B. Effects of Electric and Magnetic Field on Freezing Characteristics of Gel Model Food. Food Research International, 2023, 166, 112566. https://doi.org/10.1016/j.foodres.2023.112566
44. Jiang, S.; Zhao, S. C.; Jia, X. W.; Wang, H.; Zhang, H.; Liu, Q.; Kong, B. H. Thermal Gelling Properties and Structural Properties of Myofibrillar Protein Including Thermo-reversible and Thermo-irreversible Curdlan Gels. Food Chemistry, 2020, 311, 126018. https://10.1016/j.foodchem.2019.126018
45. Xu, L.; Wang, J.; Lv, Y.; Su, Y.; Chang, C.; Gu, L.; Yang, Y.; Li, J. Influence of Konjac Glucomannan on the Emulsion-filled/Non-filled Chicken Gel: Study on Intermolecular Forces, Microstructure and Gelling Properties. Food Hydrocolloids, 2022, 124, 107269. https://doi.org/10.1016/j.foodhyd.2021.107269
46. Farouk, M. M.; Wieliczko, K.; Lim, R.; Turnwald, S.; Macdonald, G. A. Cooked sausage Batter Cohesiveness as Affected by Sarcoplasmic Proteins. Meat Science, 2002, 61(1), 85-90. https://10.1016/s0309-1740(01)00168-1
47. Zhu, Z. W.; Lanier, T. C.; Farkas, B. E. High Pressure Effects on Heat-induced Gelation of Threadfin Bream (Nemipterus spp.) Surimi. Journal of Food Engineering, 2015, 146, 23-27. https://10.1016/j.jfoodeng.2014.08.021

 doi:10.20944/preprints202502.1353.v1